High Resolution Cerebral Perfusion Deconvolution via Mixture of Gaussian Model based on Noise Properties

Sui Li[a,b], Zhaoying Bian[a,b], Dong Zeng[a,b], Jianhua Ma*[a,b]
[a]School of Biomedical Engineering, Southern Medical University, Guangzhou, China; [b]Guangdong Artificial Intelligence and Digital Economy Laboratory (Guangzhou), Guangdong, China.

ABSTRACT

Cerebral perfusion computed tomography (CPCT) imaging provides a rapid and accurate noninvasive measurements of the acute stroke by generating hemodynamic parameter maps with a qualitative and quantitative way. However, due to it performs a multiple consecutive scanning protocol at one area of the head, the radiation exposure is relatively higher than a routine protocol. And lowering radiation dose in CPCT protocol would increase the amount of noise and hence influence hemodynamic parameters for patients with acute stroke. Some advanced methods have been proposed and show a great potential in noise suppression for low-dose CPCT imaging. And most of them assume that the embedded noise obeys an independent and identically distribution (i.i.d), but the noise may be more complicated in practical scenarios. In this work, we first analysze the noise properties in low-dose CPCT images. And then present a novel perfusion deconvolution method with a self-relative structure similarity information and a mixture of Gaussians (MoG) noise model (named SR-MoG) to accurately estimate the hemodynamic parameters directly at the low radiation exposure. Experiments implemented on digital brain perfusion phantom verify that the presented SR-MoG method can achieve promising gains over the existing deconvolution approaches.

Keywords: Cerebral perfusion CT, mixture of Gaussian model, noise properties, deconvolution.

1. INTRODUCTION

Cerebral stroke is an acute cerebrovascular disease, it has a high incidence rate, high mortality rate, and high disability rate[1]. Cerebral perfusion computed tomography (CPCT) is an imaging modality that provides detailed information about blood flow to the brain in a rapid, noninvasive, and quantitative way for cerebral stroke diagnosis. Specifically, the CPCT measures the temporal changes for each voxel through a series of repeating CT scanning, which is used to improve detection of acute infarction and help assess the degree of collateral circulation by providing hemodynamic parameters maps (HPMs), i.e., cerebral blood flow (CBF), cerebral blood volume (CBV), and mean transit time (MTT)[2]. However, CPCT performs repeated scans on the same region, so it is associated with high radiation dose. And lowering radiation dose in CPCT imaging would increase the amount of noise and hence influence HPMs' accuracy.

To reduce radiation dose in CPCT imaging while maintaining HPMs' accuracy, various algorithms have been proposed. Generally, related algorithms can be grouped into two categories. The first category is to reduce noise in the reconstructed CPCT images at low-dose measurements and to estimate HPMs via standard deconvolution process[3-5], e.g., image-based restoration algorithms, statistical iterative reconstruction algorithms. However, since noise distribution characteristics are not considered accurately, these methods might suffer from resolution loss, thereby degrading the HPMs' accuracy. The second category is to directly calculate HPMs via design strong prior information to stable the residue function with an iterative deconvolution procedure[6,7]. These models can improve the HPMs' accuracy in the case of low-dose measurement. However, most of models are based on the assumption that the embedded noise in the CPCT images is an independent and identically distribution, and this would deviate from the practical scenarios wherein the noise distributions among different frames could be significantly different from each other.

* Further author information: (Send correspondence to J. M.)

J. M. E-mail: jhma@smu.edu.cn

7th International Conference on Image Formation in X-Ray Computed Tomography,
edited by Joseph Webster Stayman, Proc. of SPIE Vol. 12304, 1230422
 · 0277-786X · doi: 10.1117/12.2646643

Therefore, supposing the noise in CPCT imaging is complex and does not obey an i.i.d, in this work, we present a novel framework to estimate HPMs by characterizing the noise distribution properly. Specifically, a non-independent and identically distributed mixture of Gaussians (MoG) noise model is utilized to modeling the residue function in the perfusion deconvolution procedure. In addition, we introduce the self-relative structure similarity information of CPCT images as a prior term, which can be easily integrated into the MoG model to further improve the HPMs' results. Finally, the fast iterative shrinkage-thresholding algorithm (FISTA) [8] is developed to solve this model. The experimental results of the digital brain perfusion phantom simulation demonstrate the presented algorithm can greatly achieve promising gains over the existing deconvolution approaches.

2. METHODOLOGY

2.1 The noise properties for low-dose CPCT image

Fig. 1 shows the normal-dose CPCT images, the low-dose CPCT images, and the corresponding difference maps at three different frames (the 1st, 12th, and 20th frames, respectively). As depicted in Fig. 1(d), it shows the corresponding histograms of the noise maps in Fig. 1(c). It can be observed that the peak of histogram at the 12th frame is lower than those at the 1th and 20th frames. The possible reason is that the 12th frame contains more contrast than the other frames, and it would suffer much more noise-induced artifacts due to the contrast agent. Fig. 2 further illustrates the different types of noise at different areas at a single frame. It can be observed that different areas contains different noise distribution at a single frame. Therefore, it can be concluded that the noise distribution in low-dose CPCT images is complex, and in this work, we exploit the mixture of Gaussian (MoG) to model the noise E of low-dose CPCT image as follows:

$$P_E(E|\Pi,\Sigma) = \sum_{k=1}^{K} \pi_k \mathcal{N}(E|0,\Sigma_k), \tag{1}$$

where $\pi_k \geq 0$ is the mixing coefficient with $\sum_k \pi_k = 1$. And $\mathcal{N}(\cdot|0,\Sigma_k)$ represents a Gaussian distribution with zero mean and variance Σ_k.

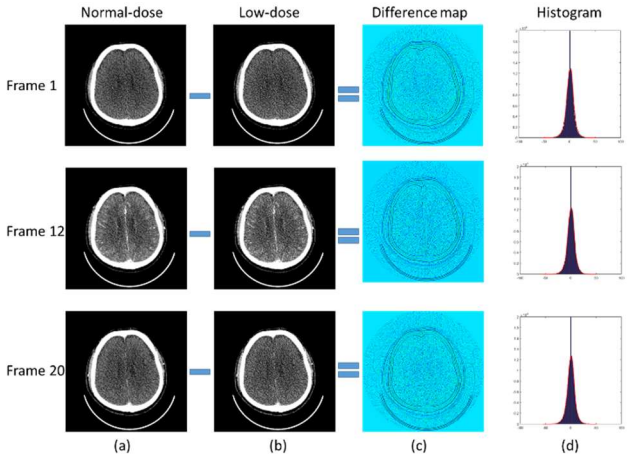

Figure 1. Installation of (a) the normal-dose CPCT images at frame 1, 12 and 20, (b) the low-dose CPCT images at frame 1, 12 and 20, (c) the difference images from (a) and (b), and (d) the histogram map of the difference images from (c)..

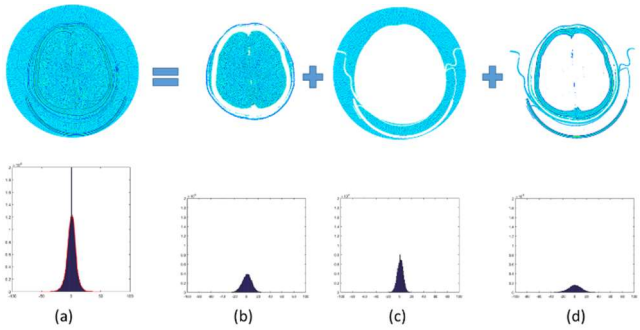

Figure 2. (a) Illustration of the noise at the 12th CPCT frame and its histogram. (b)-(d) Illustration of three different Gaussian components and their histograms, obtained by MoG model with three Gaussian components of the noise in (a).

2.2 SR-MoG deconvolution model

The CPCT images can be considered as the combination of the background component with temporal similarity and the foreground component with spatial contiguity and noise [9]. Meanwhile, the concentration maps are obtained by subtracting the baseline image wherein the baseline image equals the average of early CPCT frames before the contrast agent enters the blood vessel actually. Moreover, the residue function data reflects the relative concentration of contrast agent in the blood vessels over time. Therefore, it can be concluded that the residue function can also be considered as the combination of the background component and foreground component as well. Motivated by these observations, the residue function data X consists of background component U, foreground component F, and embedded noise component E, which can be modeled as follows:

$$X = U + F + E \tag{2}$$

According to Eq. (2) and the noise model in Eq. (1), we can obtain following likelihood distribution for U and F:

$$\begin{aligned} P_X(X|U,F,\Pi,\Sigma) &= P_E(X-U-F|\Pi,\Sigma) \\ &= \sum_{k\&=1}^{K} \pi_k \mathcal{N}(X-U-F|0,\Sigma_k) \end{aligned} \tag{3}$$

To estimate the underlying variable U, we introduce a we introduce self-relative information B to provide prior information for U, , then, we provide following prior distribution for U:

$$P_U(U) = \mathcal{N}(U|B,\sigma_1) \tag{4}$$

where σ_1 denotes the variance of the inevitable noise in B.

Moreover, since the foreground component F is variant and sparse over time, it is rational to introduce a sparse prior distribution $P_F(F)$ on it. This prior can be express as a regularization term when estimating F. By combining the priors and the likelihood in Eq. (4), it can be then expressed as following posteriori distribution:

$$P(U,F,\Pi,\Sigma|X) \propto P_X(X|U,F,\Pi,\Sigma) \times P_U(U) \times P_F(F) = \sum_k \pi_k \mathcal{N}(X-F-U|0,\Sigma_k) \times \mathcal{N}(U|B,\sigma_1) \times P_F(F) \tag{5}$$

Therefore, by integrating the perfusion deconvolution procedure with the likelihood model as aforementioned, the perfusion deconvolution model can be rewritten as:

$$\hat{X} = \operatorname{argmin} \frac{1}{2}\|AX-C\|_2^2 + \log \sum_{k=1}^{K} \pi_k \mathcal{N}(X-U-F|0,\Sigma_k) + \log N(U|B,\sigma_1) + \beta \log P_F(F)$$

$$s.t. X = U + F + E \tag{6}$$

where the $\log P_F(F) = \|D(F)\|_F^2$ and the operator $D(\cdot)$ is the first order difference matrix. Then we can estimate the underlying background and foreground, as well as other involved parameters. By incorporating the self-relative structural similarity information and MoG noise distribution latent in CPCT images into a perfusion deconvolution model, we can define the self-relative structural-information-induced mixture of Gaussian (SR-MoG) model.

3. EXPERIMENTS

3.1 Data

To validate and evaluate the performance of the presented SR-MoG perfusion deconvolution model at low-dose cases, a digital brain perfusion phantom package [10] was used in this work. The specific digital brain perfusion phantom consists of infarct core and ischemic penumbra in the white and gray matters, as well as the healthy tissue with 40 temporal frames at size 256 × 256. Fig. 3 shows the phantom and the corresponding time-density curves of penumbral, strike core, tissue and vessel. Additionally, to simulate low-dose CPCT images under different dose levels, the simulate strategy is based on the previous study [11], and two dose levels were simulated with 50% and 25% of normal-dose.

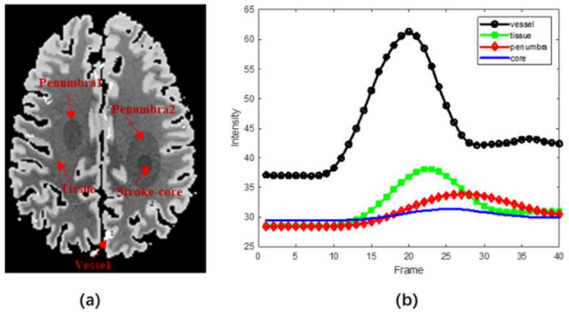

Figure 3. Illustration of digital CPCT phantom (a) and the corresponding TDCs (b). The display window is [10, 65] HU.

3.2 Comparison methods

To validate and evaluate the performance of the presented SR-MoG method, five deconvolution methods were compared against: block-circulant truncated SVD (bSVD) [12], Tikhonov regularization [13], the tensor total variation regularized approach (TTV) [6], the structure total variation regularized approach (STV) [7] and the SR-MoG with a single Gaussian noise component (SG). Extensive experiments with different parameter settings were conducted for all competing methods, and the appropriate parameters are selected based on the optimal visual inspection.

4. RESULT

Fig. 4 shows the estimated HPMs, i.e., CBF, CBV, and MTT generated by different algorithms of digital brain perfusion phantom with 50% dose level. The reference HPMs obtained by the digital brain perfusion phantom package directly, thus it can be as the "golden standard" in this comparison. The remaining HPMs all estimated from the FBP reconstructed low-dose CPCT images by the competing deconvolution methods for comparison. It can be observed that several noise is evident in the traditional deconvolution methods, i.e., bSVD, Tikhonov, especially in healthy region of brain. And for the TTV and STV algorithms, the results shows more improvement by visual inspection, while the detailed structure of the stroke-core region is still corrupted by the noise-induced artifacts, as shown by the red arrows at CBF maps in Fig. 4. Moreover, the results from SG and SR-MoG are remarkable over that from TTV and STV in terms of noise reduction and structure information preservation. However, by careful visual inspection, the values of SG at penumbra region, indicated by yellow arrows in Fig. 4, are lighter than that in reference, and results of SR-MoG are closer than other deconvolution approach.

Fig. 5 illustrates the performance of all competing methods on digital phantom with 25% dose, respectively. With the radiation dose further reducing, all compared methods fail to remove all noise, especially at 25% dose. While the presented SR-MoG performed better than other compared methods in terms of noise suppression, structure preservation and value

consistency, especially for the penumbra and stroke-core regions.

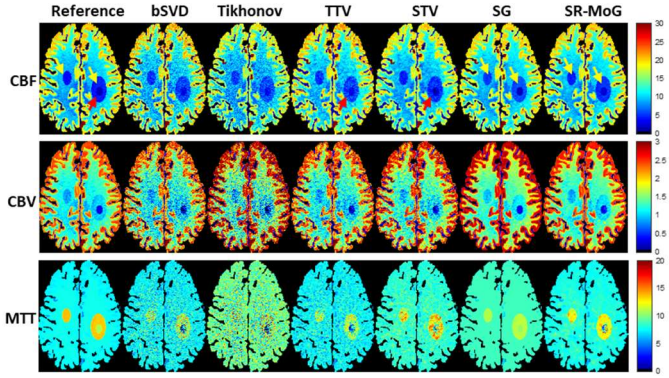

Figure 4. Perfusion maps of the digital brain perfusion phantom estimated by bSVD, Tikhonov, TTV, STV, SG and SR-MoG approaches, respectively, under the 50% dose. CBF in unit of mL/100 g/min, CBF in mL/100 g, MTT in sec.

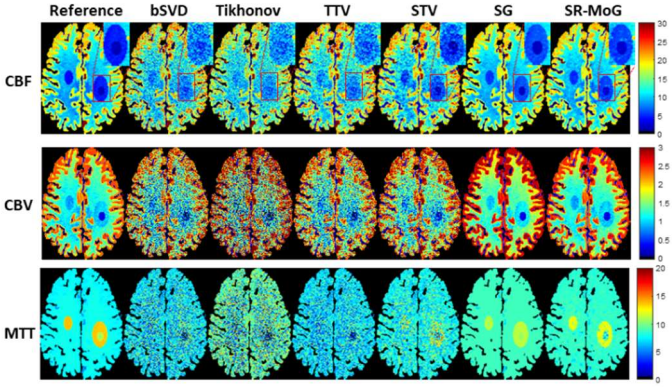

Figure 5. Perfusion maps of the digital brain perfusion phantom estimated by bSVD, Tikhonov, TTV, STV, SG and SR-MoG approaches, respectively, under the 25% dose. CBF in unit of mL/100 g/min, CBF in mL/100 g, MTT in sec.

Table 1. RMSE and SSIM for HPMs (CBF, CBV, MTT) estimated using the different competing methods at 25% and 50% of normal dose. Bold font indicates the best performance.

		CBF		CBV		MTT	
Methods	Dose	RMSE	SSIM	RMSE	SSIM	RMSE	SSIM
bSVD	25%	2.9152	0.9123	0.4537	0.9955	2.4328	0.9213
Tikhonov		4.6676	0.9143	1.8534	0.9790	3.4193	0.8510
TTV		2.8414	0.9236	0.4288	0.9960	2.3473	0.9301
STV		2.9210	0.9502	0.5705	0.9944	1.7319	0.9564
SG		2.0843	0.9978	0.5974	0.9946	2.9620	0.9321
SR-MoG		**1.9456**	**0.9963**	**0.1405**	**0.9990**	**1.6187**	**0.9718**
bSVD	50%	1.4844	0.9741	0.2280	0.9988	1.3656	0.9730
Tikhonov		4.1308	0.9690	1.7753	0.9849	2.6510	0.9158
TTV		1.2916	0.9828	0.2190	0.9990	1.3018	0.9765
STV		1.7399	0.9868	0.4508	0.9969	1.2121	0.9793
SG		1.0834	0.9978	0.5960	0.9947	11.1994	0.8917
SR-MoG		**0.7962**	**0.9988**	**0.1616**	**0.9990**	**0.8843**	**0.9889**

To further demonstrate the performance of the presented SR-MoG method, RMSE and SSIM measurements are utilized and corresponding comparison results of the different methods at 50% dose and 25% dose, and the result is listed in Table. 1. It can be seen that the presented SR-MoG method outperforms the other competing methods by a large margins in terms of the RMSE and SSIM measurements at the two dose levels. Thus results demonstrate the presented SR-MoG deconvolution algorithm achieve significant ability compared with other algorithm for noise suppression and structure consistent.

ACKNOWLEDGMENT

This work was supported in part by the NSFC under Grant U21A6005 and Grant U1708261, the National Key R&D Program of China under Grant No. 2020YFA0712200, and Young Talent Support Project of Guangzhou Association for Science and Technology.

REFERENCES

[1] B. C. V. Campbell, D. A. De Silva, M. R. Macleod, S. B. Coutts, L. H. Schwamm, S. M. Davis, and G. A. Donnan, "Ischaemic stroke," Nature Reviews Disease Primers, vol. 5, no. 1, p. 70, 2019.

[2] A. Konstas, G. Goldmakher, T.-Y. Lee, and M. Lev, "Theoretic basis and technical implementations of CT perfusion in acute ischemic stroke, part 2: Technical implementations," American Journal of Neuroradiology, vol. 30, no. 5, pp. 885–892, 2009.

[3] S. Li, D. Zeng, J. Peng, Z. Bian, H. Zhang, Q. Xie, Y. Wang, Y. Liao, S. Zhang, J. Huang, D. Meng, Z. Xu, and J. Ma, "An efficient iterative cerebral perfusion CT reconstruction via low-rank tensor decomposition with spatial–temporal total variation regularization," IEEE Transactions on Medical Imaging, vol. 38, pp. 360–370, 2019.

[4] S. Li, D. Zeng, Z. Bian, D. Li, M. Zhu, J. Huang, and J. Ma, "Learning non-local perfusion textures for high-quality computed tomography perfusion imaging," Physics in Medicine & Biology, vol. 66, no. 11, p. 115007, 2021.

[5] J. Ma, H. Zhang, Y. Gao, J. Huang, Z. Liang, Q. Feng, and W. Chen, "Iterative image reconstruction for cerebral perfusion CT using a precontrast scan induced edge-preserving prior," Phys. Med. Biol., vol. 57, pp. 7519-7542, 2012.

[6] R. Fang, S. Zhang, T. Chen, and P. Sanelli, "Robust low-dose CT perfusion deconvolution via tensor total-variation regularization," IEEE Transactions on Medical Imaging, vol. 34, 2015.

[7] D. Zeng, X. Zhang, Z. Bian, J. Huang, H. Zhang, L. Lu, W. Lyu, J. Zhang, Q. Feng, W. Chen, and J. Ma, "Cerebral perfusion computed tomography deconvolution via structure tensor total variation regularization." Medical Physics, vol. 43, pp. 2091-2107, 2016.

[8] A. Beck and M. Teboulle, "A fast iterative shrinkage-thresholding algorithm for linear inverse problems," SIAM journal on imaging sciences, vol. 2, no. 1, pp. 183–202, 2009.

[9] D. Zeng, Q. Xie, W. Cao, J. Lin, H. Zhang, S. Zhang, J. Huang, Z. Bian, D. Meng, Z. Xu, Z. Liang, W. Chen, and J. Ma, "Low-dose dynamic cerebral perfusion computed tomography reconstruction via kroneckerbasis-representation tensor sparsity regularization," IEEE Transactions on Medical Imaging, vol. 36, pp. 2546–2556, 2017.

[10] https://lme.tf.fau.de/dataset/digital-brain-perfusion-phantom

[11] J. Ma, Z. Liang, Y. Fan, Y. Liu, J. Huang, W. Chen, and H. Lu, "Variance analysis of x-ray CT sinograms in the presence of electronic noise background," Medical Physics, vol. 39, no. 7Part1, pp. 4051–4065, 2012.

[12] O. Wu, L. Østergaard, R. M. Weisskoff, T. Benner, B. R. Rosen, and A. G. Sorensen, "Tracer arrival timing-insensitive technique for estimating flow in MR perfusion-weighted imaging using singular value decomposition with a block-circulant deconvolution matrix.," Magnetic Resonance in Medicine, vol. 50, pp. 164–74, Jul 2003.

[13] T. S. Koh, X. Y. Wu, L. H. Cheong, and C. C. T. Lim, "Assessment of perfusion by dynamic contrast-enhanced imaging using a deconvolution approach based on regression and singular value decomposition," IEEE Transactions on Medical Imaging, vol. 23, no. 12, pp. 1532–1542, 2004.